CALCULATING PATIENT SPECIFIC DOSES IN X-RAY DIAGNOSTICS AND FROM RADIOPHARMACEUTICALS

Juha Lampinen

Department of Physics
Faculty of Science
University of Helsinki
Helsinki, Finland

ACADEMIC DISSERTATION

*To be presented, with the permission of
the Faculty of Science of the University of Helsinki,
for public criticism in Auditorium FI of
the Department of Physics
on March 18 th, 2000, at 10 o'clock.*

Helsinki 2000

ABSTRACT

The risk associated with exposure to ionising radiation is dependent on the characteristics of the exposed individual. The size and structure of the individual influences the absorbed dose distribution in the organs. Traditional methods used to calculate the patient organ doses are based on standardised calculation phantoms, which neglect the variance of the patient size or even sex. When estimating the radiation dose of an individual patient, patient specific calculation methods must be used. Methods for patient specific dosimetry in the fields of X-ray diagnostics and diagnostic and therapeutic use of radiopharmaceuticals were proposed in this thesis.

A computer program, ODS-60, for calculating organ doses from diagnostic X-ray exposures was presented. The calculation is done in a patient specific phantom with depth dose and profile algorithms fitted to Monte Carlo simulation data from a previous study. Improvements to the version reported earlier were introduced, e.g. bone attenuation was implemented. The applicability of the program to determine patient doses from complex X-ray examinations (barium enema examination) was studied. The conversion equations derived for female and male patients as a function of patient weight gave the smallest deviation from the actual patient doses when compared to previous studies.

Another computer program, Intdose, was presented for calculation of the dose distribution from radiopharmaceuticals. The calculation is based on convolution of an isotope specific point dose kernel with activity distribution, obtained from single photon emission computed tomography (SPECT) images. Anatomical information is taken from magnetic resonance (MR) or computed tomography (CT) images. According to a phantom study, Intdose agreed within 3 % with measurements. For volunteers administered diagnostic radiopharmaceuticals, the results given by Intdose were found to agree with traditional methods in cases of medium sized patients. For patients undergoing systemic radiation therapy, the results by Intdose differed from measurements due to dynamic biodistribution of the radiopharmaceutical since the calculation was based only on one set of SPECT images.

In general, traditional methods using average sized calculation phantoms are intended to give average doses for an exposed population. For calculating doses to individual patients, patient specific calculation methods, e.g. ones proposed in this thesis, should be used.

CONTENTS

LIST OF PUBLICATIONS

This thesis is based on the following original publications, which are referred to in the text by their Roman numerals, Publ. I-V.

I   Rannikko S, Ermakov I, Lampinen JS, Toivonen M, Karila KTK, Chervjakov A. Computing patient doses of X-ray examinations using a patient size- and sex-adjustable phantom. British Journal of Radiology 1997; 70: 708-718.

II   Lampinen JS, Rannikko S. Patient specific doses used to analyse the optimum dose delivery in barium enema examinations. British Journal of Radiology 1999; 72: 1185-1195.

III   Vehmas T, Lampinen JS, Mertjärvi A, Rannikko S. Factors influencing patient radiation doses from barium enema examinations. Acta Radiologica 2000; 41: 167-171.

IV   Lampinen JS, Pohjonen HK, Savolainen SE. Calculating internal dose by convolution from SPECT/MR fusion images. Annals of Nuclear Medicine 1998; 12: 1-5.

V   Aschan AC, Toivonen MJ, Lampinen JS, Tenhunen M, Kairemo KJA, Korppi-Tommola ET, Jekunen AP, Sipilä P, Savolainen SE. The use of TL detectors in dosimetry of systemic radiation therapy. Acta Oncologica 1999; 38: 189-196.

NOMENCLATURE

A	Activity [Bq]
AP	Anteroposterior projection
ALARA	As low as reasonably achieved
BEIR	Committee on the Biological Effects of Ioninizing Radiation
CT	Computed tomography
DAP	Dose-area product [$Gy \cdot cm^2$]
E	Effective dose [Sv]
ε	Effective individual dose [Sv]
E_p	Photon energy [eV]
EC	European Commission
EGS4	Electron-Gamma Shower v. 4
ESD	Entrance surface dose [Gy]
FFT	Fast Fourier transform
gcc	Gnu Project C Compiler
HVL	Half value layer
ICRP	International Commission on Radiological Protection
in vivo	In the living thing (Latin)
K_a	Air kerma (kinetic energy released in matter) [Gy]
LAT	Lateral projection
MCNP	A General Monte Carlo N-Particle Transport Code
MIRD	Medical Internal Radiation Dose Committee
MoAb	Monoclonal antibody
MR	Magnetic resonance
PA	Posteroanterior projection
PCXMC	PC program for X-ray Monte Carlo
ROI	Region of interest
SPECT	Single photon emission computed tomography
SRT	Systemic radiation therapy
TL	Thermoluminescent
VMC	The Voxel Monte Carlo Code

AIM OF THE STUDY

The aim of this thesis is to describe methods developed for patient specific radiation dose calculations and to demonstrate their use in clinical X-ray examinations and nuclear medicine applications.

The specific aims of the thesis are:

1) to develop a computer application using a patient size- and sex-adjustable phantom for calculating patient specific organ doses from X-ray examinations,

2) to demonstrate the use of the developed application for investigating patient doses, presenting barium enema examination as an example,

3) to develop a computer application using SPECT/MR fusion images and the convolution method for calculating patient specific dose distributions for patients administered radiopharmaceuticals,

4) to apply the developed computer program for calculating dose distributions in patients undergoing systemic radiation therapy.

1 INTRODUCTION

The knowledge of the absorbed radiation dose to the organs of a patient undergoing a procedure involving radiation is essential in order to evaluate the detriment of the procedure. The knowledge of the detriment is needed to evaluate the net benefit from the procedure. The net benefit shall be sufficient in order to regard the exposure as justified (ICRP 1991, EC 1997). In addition to the requirement of net benefit, the exposures should be optimised, i.e. the magnitude of individual doses should be kept as low as reasonably achieved (ALARA). The ALARA principle has different interpretations in diagnostics and therapy. In diagnostics, the ALARA principle means that the radiation burden to the patient should be as low as reasonably achieved consistent with obtaining the required diagnostic information (EC 1997). In radiation therapy, exposures of target volumes shall be individually planned and the doses of non-target volumes and tissues shall be optimised to be as low as reasonably achieved (EC 1997).

The desired quantity in patient dosimetry is the absorbed dose distribution in the patient. Because of practical reasons mean absorbed doses to organs, i.e. organ doses are used. According to present understanding, the radiation-induced detriment can be assessed from the known organ doses (ICRP 1991). In current European legislation (EC 1997) the quantity describing overall risk from exposure to radiation is the effective dose, E [Sv] (ICRP 1991). E is determined from organ doses and organ specific, radiation risk related, weighting factors. The weighting factors of the effective dose are derived as an average for the whole population. The weighting factors and the rules for using them are based on scientific data, available mainly from atom bomb survivors in Hiroshima and Nagasaki. The International Commission on Radiological Protection (ICRP) has issued the latest definition of the weighting factors in 1995 (ICRP 1995). In addition to tissue weighting factors, the effective dose also includes radiation quality factors. Different radiation qualities induce different biological effects as the radiation interacts with tissues. For photon radiation the quality factor is unity (ICRP 1991).

The Committee on the Biological Effects of Ioninizing Radiation (BEIR), assigned by the National Research Council in USA, has published reports about the health effects of ionising radiation. The latest report is known as BEIR V (BEIR 1990). The committee has not given a quantity comparable to E, but they sum up organ and tissue specific risk assessments. Important aspects of these risk assessments are the sex and age of the individuals. The methodology presented in BEIR V may be used to calculate a statistical estimate of fatal cancer cases caused by exposures to radiation if the organ doses and age distribution of the exposed individuals and local cancer and life expectancy statistics are available.

In routine radiological procedures, it is not practical to conduct *in vivo* measurements of organ doses. The possible practical methods for deriving the organ doses are measurements in a phantom (see e.g. Toivonen et al. 1996), i.e. an artificial object representing a patient, or computer calculations. An important method applicable to a wide range of applications is Monte Carlo simulation, which was introduced for the first time

by Buffon in 1777 to estimate the value of π (Schroeder 1974). The Monte Carlo simulation has been widely adopted to radiation physics (for its applications in medical radiation physics, see e.g. Andreo 1991). In a radiation physics simulation a virtual image of the exposure conditions is modelled to a computer program, which then creates virtual radiation particles and simulates interactions between the particles and the medium. The particle tracks are followed from the source to their final absorption. Possible interactions with matter are induced with random numbers and known probabilities of each interaction type. The Monte Carlo simulation method itself is well documented and verified against measurements. Several Monte Carlo application packages are readily available. The present choices of the research community include e.g. EGS4 (Electron-Gamma Shower) by Nelson et al. (1985), MCNP (A General Monte Carlo N-Particle Transport Code) (Briesmeister 1997) and VMC (The Voxel Monte Carlo model) (Kawrakov et al. 1996) applications, for which the user provides their own geometry and sources. The packages provide the algorithms needed for radiation transport simulation.

Monte Carlo simulation is the established method for determining patient radiation doses both in X-ray and nuclear medicine diagnostics. The basic phantom model used in these simulations is the hermaphrodite MIRD (Medical Internal Radiation Dose Committee, assigned by the Society of Nuclear Medicine) phantom, originally developed for use in estimates of internal dose (Snyder et al. 1969). The body contour and the organs of the MIRD phantom are defined with geometrical shapes. The MIRD phantom has since been improved, i.e. new organs have been included (Jones et Wall 1985) and sexes have been separated (Kramer et al. 1982). Special phantoms have been developed to model children at different ages (Cristy 1980). The basic concepts of all these modifications to the MIRD phantom are similar to each other, they are all based on mathematical shapes. In addition to mathematical phantoms, phantoms based on actual human anatomical data from computed tomography (CT) or magnetic resonance (MR) images may also be used in Monte Carlo simulations (Tagesson et al. 1996, Furhang et al. 1996a, Furhang et al. 1997, du Plessis et al. 1998).

The use of the Monte Carlo method for organ dose calculation in X-ray diagnostics was introduced by Rosenstein, who using a MIRD based phantom calculated doses to five organs for adult (Rosenstein 1976) and paediatric (Rosenstein et al. 1979) X-ray examinations. Drexler et al. (1984) used the sex-specific phantoms of Kramer et al. (1982) to calculate organ doses in conventional X-ray examinations. Jones et Wall (1985) used their phantom to calculate organ doses in 12 common X-ray examinations. Hart et al. (1994) determined conversion coefficients from entrance surface dose (*ESD*) and dose-area product (*DAP*) to organ doses using an improved phantom which included all the organs needed for calculating the effective dose (ICRP 1991). They also presented conversion coefficients from the total *DAP* value of an examination for nine complex X-ray examinations composed of several exposures; for example a coefficient of 0.28 mSv/Gy·cm^2 was given for barium enema examination. Hart et al. (1996) have also calculated conversion coefficients for estimating effective doses in paediatric X-ray

examinations. Several front-end applications have been developed to simplify the use of the conversion coefficient tables (e.g. EFFDOSE and CHILDOS[1]).

Monte Carlo simulation is time consuming. It is therefore practical to use pre-calculated conversion coefficients from an easily measurable quantity to effective dose or organ doses. In X-ray diagnostics this measurable quantity may be entrance surface dose, ESD [Gy], air kerma, K_a [Gy] or dose-area product, DAP [Gy·cm^2]. In diagnostic nuclear medicine administered activity, A [Bq], is used. The conversion coefficients are derived for a phantom representing an average patient. Therefore, the organ doses determined with conversion coefficients represent average doses for a large population, which in fact are needed to calculate the effective dose as defined by ICRP.

The conversion coefficients apply only to the pre-calculated conditions, i.e. exposure geometry, radiation spectra and patient size. The end-user is able to estimate the organ and effective doses without using the Monte Carlo application itself. Tapiovaara et al. (1997) have presented a more flexible Monte Carlo application, in which the end-user is able adjust the exposure geometry, radiation spectra and patient size. The basic phantom is selected from six mathematical hermaphrodite phantoms (adult, 15, 10, 5 or 1-year old) by Cristy (1980), which may then be adjusted in size according to the patient in question. The results of the time consuming radiation transport simulation of one particular exposure geometry may be used to calculate organ doses for any spectra, which makes it simple to compare the effects of different radiation qualities.

In dosimetry of nuclear medicine where absorbed doses to organs from radiation emitting from internal sources are of interest, the calculation is based on S-values. The methodology was originally developed by Loevinger et Berman (1968) and it was implemented to practice in a MIRD pamphlet (Snyder et al. 1975). Traditionally an S-value describes the absorbed dose to a specific target organ from radiation emitting from another specific source organ. An S-value defined at the organ level assumes that the activity inside the source organ is homogeneously distributed. The organ level S-values are derived using Monte Carlo methods and MIRD phantom. S-values have recently been developed to be applicable also to dosimetry at the suborgan, voxel, multicellular and cellular levels (Howell et al. 1999, Bolch et al. 1999). Organ level S-values for common radiopharmaceuticals used in nuclear medicine diagnostics are published by ICRP (1987). The data has been calculated assuming that the biodistribution of the radiopharmaceuticals in the patients, i.e. the distribution of the injected substance in the organs and tissues, behaves as for an average human. Patient specific properties of the biodistribution are ignored. Several computer applications have been developed to simplify the use of S-values, i.e. MABDOS (Johnson 1988) and MIRDOSE3 (Stabin 1996).

Different approaches to the use of Monte Carlo simulations to benefit patient dose calculations are demonstrated in Publ. I and IV. In Publ. I analytical algorithms are fitted to dose distribution data from extensive Monte Carlo simulations where a water phantom was exposed to various X-ray spectra (Tapiovaara 1983). The algorithms are then used

---

[1] Le Heron JC, National Radiation Laboratory, Christchurch, New Zealand

to calculate the dose distribution in an anatomical phantom. The anatomical phantom is sex-specific, and its size is adjusted to match the size of the patient (Servomaa et al. 1989). This technique is fast, since the results from time-consuming simulations are re-shaped to flexible equations. In Publ. IV point dose kernels describing the dose distribution from a point source for selected isotopes were convoluted with the activity distribution to get the absorbed dose distribution. The activity distribution is obtained from SPECT (single photon emission computed tomography) images of the patient in question. The organ doses of the patient were derived from the absorbed dose distribution using MR (magnetic resonance) images for the patient's anatomical information. The convolution process is again fast compared to the simulation and verified kernels are available in the literature (Furhang et al. 1996b).

The use of the methods introduced in Publ. I and IV are demonstrated in Publ. II, III and V. Patient specific organ and effective doses of 89 barium enema X-ray examination patients are calculated as an example of the capabilities of the computer program described in Publ. I. In addition to reporting the calculated doses in Publ. II and III, new aspects of analysing dose delivery (Publ. II) and factors influencing the patient dose (Publ. III) are considered. In Publ. V the computer program introduced in Publ. IV is applied to calculate dose distributions and doses to some organs of six patients undergoing systemic radiation therapy (SRT). The doses calculated with the patient specific method and input data are compared with the doses calculated with conversion coefficients. Some unpublished methods and results are also presented. Improvements to the computer program described in Publ. I are reported.

2   COMPUTING PATIENT RADIATION DOSES IN X-RAY DIAGNOSTICS

A computer program, later referred to as ODS-60[2], which is able to calculate patient specific organ doses from X-ray examinations was developed (Publ. I). ODS-60 is a combination of two modules, a size- and sex-adjustable phantom model and a collection of algorithms to calculate the absorbed dose to an arbitrary point in the phantom. The program code was written in standard C language and compiled with Gnu Project C Compiler (gcc). A user interface (Lampinen et al. 1996) was developed with Visual Basic 4.0[3].

The phantom model (Servomaa et al. 1989) is based on an anatomical Alderson-Rando phantom[4] and an anatomical atlas (Symington 1956). The basic phantom represents a male of 173 cm in height and 73.5 kg in weight. The phantom is constructed from slices, for which the body and organ contours are described with points. A line connecting the points of each shape defines the contour of that shape. The co-ordinates of each point are transformed to correspond to the patient's size. A female phantom is constructed from the male phantom by changing the description of the chest and pelvic regions to correspond to female anatomy.

2.1 Methods

The absorbed doses to the organs in the ODS-60 program are calculated using Monte Carlo-simulated dose distributions for a semi-infinitive, 30-cm thick water slab (Tapiovaara 1983). Mathematical equations, representing relative depth dose and dose profiles, are used to calculate absorbed dose at an arbitrary point in the above mentioned semi-infinitive water slab. The phantom is positioned in the slab according to the exposure geometry, i.e. projection and position of the X-ray field on the patient's skin. The program divides the organs into 1 cm · 1 cm · z cm (z being the slice thickness) sized voxels for which the absorbed doses are calculated. The organ dose is the average absorbed dose in the voxels of an organ. The effective dose is calculated using the ICRP weighting factors, but since the phantom is sex-specific, ovary, uterus and breast doses are available only to females and testis dose only to males. The absorbed dose to the fetus is not calculated, but may in the early stages of pregnancy be estimated from the uterus dose.

All materials in the phantom, in the program version reported in Publ. I, are assumed to be water with the exception of lung tissue. The lung tissue is assumed to be otherwise similar to water, but only 0.3 g/cm^{3} in density. Therefore, an adjusted depth value is used in the depth dose and dose profile equations in the case of a voxel which

---

[2] Rados Technology Oy, Turku, Finland

[3] Microsoft Corporation, Redmond, Washington, USA

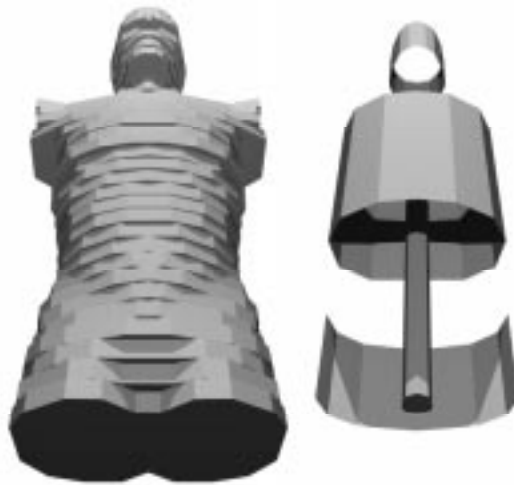[4] The Phantom Laboratory, Salem, New York, USA

Figure 1. *The body contour of the basic phantom model of the ODS-60 and the skeleton developed for him.*

has lung tissue between the voxel and focus of the X-ray tube. Also, the attenuation effect of the pelvic bone is taken into account with a correction factor, but only in the case of the uterus and ovaries.

The ODS-60 program has been further developed by the author after the first introduction in Publ. I. Several minor modifications and fixes were implemented. The backscatter factor function (equation 7 in Publ. I) was corrected to correspond to a rectangular field, as the original data by Grosswendt (1990) was derived for circular fields. The correction is done by multiplying the effective area of the field (equation 7 in Publ. I) by 0.9 (Day et Aird 1983).

The discontinuity of the backscatter factor as a function of X-ray tube voltage (shown clearly in e.g. figure 6 in Publ. I) was removed. Precisely speaking the backscatter factor is a function of the half value layer (HVL) value. The correction uses the same non-continuous functions as before, but in the vicinity of the cut-point (HVL value of 4 mm Al) an interpolation between these two functions is made.

Some organs were redefined. The contribution of the contents of the stomach, intestines and bladder to the average organ dose is no longer considered. The absorbed dose to eyes was defined separately for both eyes. The definition of the colon is selectable according to either ICRP (1991) or ICRP (1995). The density correction for lung tissue was removed.

In addition to these minor modifications, a skeleton was modelled and implemented to the ODS-60 phantom (Figure 1). The skeleton consists of a skull, spine, rib cage and pelvic bone. The properties of the skeleton have been derived from the specifications of the adult MIRD phantom (Cristy 1980) and the description of the anatomical phantom (Servomaa et al. 1989) on which the ODS-60 phantom is based. The shapes of

the bones are derived from Servomaa et al. (1989) and the thickness values from Cristy (1980). The skull covers the brain of the phantom with a 0.9-cm thick homogeneous layer. The spine was defined as an ellipse whose thickness is calculated separately for each calculation voxel (i.e. the spine thickness along the ray from X-ray focus to the voxel). The rib cage is a homogeneous 0.25-cm thick layer, derived from the 0.5-cm thick ribs of the MIRD phantom. The pelvic bone is a 0.7-cm thick arc in the posterior side of the phantom.

For simplicity, the depth dose and profile equations for the 30-cm thick water slab (from Tapiovaara (1983)) with a simple correction are used when calculating absorbed doses behind bone material. The correction method is derived from the physics of narrow beam geometry, i.e. scatter is neglected. In narrow beam geometry, the exponential attenuation equation

$$I/I_0 = exp[-(\mu/\rho) \rho t] \tag{1}$$

gives the intensity I emerging from a layer of material with thickness t and density ρ assuming an incident intensity of I_0. The mass attenuation coefficient $\mu/\rho(E_p)$ [cm^2/g] describes how a certain material attenuates primary radiation photons as a function of photon energy, E_p (Attix 1986). The depth dose equations used in ODS-60 are based on broad beam geometry simulation and the depth dose data includes knowledge about how water attenuates broad beam radiation, i.e. when a scatter component is included. The correction made for bone attenuation is based on an assumption that formalism derived for narrow beam geometry is also applicable for broad beam geometry. In practise, the correction for voxels behind bone material is implemented by recalculating the depth, t, from bone thickness t_{bone} and the actual depth of the voxel t_0 as

$$t = t_0 + \beta \, t_{bone} \tag{2}$$

where β is an experimental coefficient given as a function of X-ray spectrum. Two parameters are embedded in β, the difference of μ/ρ of water to that of bone (Hubbell et Seltzer 1997) and the ratio of the densities of bone and water (1.50) (Cristy 1980). The difference in μ/ρ is due to the different atomic composition of the two substances and it is a function of photon energy. The coefficient β was derived from dose distributions produced with Monte Carlo simulations.

An MCNP (Briesmeister 1997) application was used to simulate dose distribution in water with and without a slice of bone of variable thickness (5, 10 or 20 mm). Mono-energetic (20, 30, 40, 50, 60, 70, 80, 90 and 100 keV), non-divergent, 15 x 15 cm sized photon beams were directed towards a cubical (30 x 30 x 30 cm) phantom. The phantom consisted of either pure water or of water and a layer of bone material at a depth of 10 mm in the phantom, measured from the direction of the beam entrance. Depth dose distribution was recorded in 1 x 1 x 1 cm sized voxels using a pulse height tally *F8 [MeV] (Briesmeister 1997).

A specific value of β, $β_i$, was derived for each monoenergetic (energy E_i) photon beam. Each $β_i$ value was derived by first fitting a rational function to the simulated depth dose curve (without bone) and then finding the required horizontal shift for that curve in order to produce a curve similar to the depth dose curve simulated with the 10 mm-thick bone layer. The amount of horizontal shift was optimised to give an average ratio of 1.00 for the depth dose curves (the one simulated with bone and the one produced with the shift) in the depths from 3 cm to the tenth value layer thickness. The sum of $β_i$ over all energies E_i of the X-ray spectrum, weighted with the photon yield for each energy group is then used to calculate a value of β for an arbitrary spectrum.

The exit dose calculated by ODS-60 is defined according to narrow beam geometry. The exit dose is calculated with the exponential attenuation equation (equation 1), mass attenuation coefficients for tissue and bone (Hubbell et Seltzer 1997) and X-ray spectrum calculated for the exposure in question (Boone et Seibert 1997).

Double contrast barium enema X-ray examination is the largest single contributor (14%) to the annual collective effective dose in Finland (Rannikko et al. 1997). During the examination the patient's large intestine is first filled *per rectum* with barium contrast medium, which is then removed and replaced with air to achieve both negative and positive contrast effects. The examination procedure contains both radiographs and fluoroscopy which makes calculating the patient dose very challenging.

The patient specific organ and effective doses were derived for 89 barium enema examination patients in five hospitals in order to find out the variation in the effective dose (Publ. II) and the reasons for the variation (Publ. III). The ODS-60 program was used in the organ dose calculations. The bone correction method of the program version used in the calculations of Publ. II and III was not exactly the same as described in the previous chapter. The earlier version of the correction was based on bone thickness and an averaged photon energy effect.

Registering all the parameters required for dose calculation with ODS-60 needed the full attention of two dedicated people. The static parameters registered were patient size (length and weight) and sex and X-ray tube filtration. Parameters changing during the examination were the size (height and width), location and projection of the X-ray field, focus-skin distance, tube voltage, exposure time and current.

Due to the definition of the effective dose, i.e. it is not to be used as a radiation risk related quantity for an individual person, a new quantity, effective individual dose, $\mathcal{E}$ [Sv], was introduced in Publ. II. This new quantity is calculated as the effective dose, but the weighting factors for sex specific organs are reassigned, i.e. $\mathcal{E}$ is a sum of those organ doses and corresponding weighting factors, which are present according to patient's sex.

2.2 Results and findings

A demonstration of the abilities of the bone correction method described above is presented in figure 2. The effect of the skeleton in the exit dose, i.e. the primary part of the radiation penetrating the phantom, calculation is demonstrated in figure 3 of Publ. II.

In comparison with experimental dose determinations in an Alderson-Rando phantom with TL dosimeters (Toivonen et al. 1996), the doses calculated with ODS-60 converg towards the measured ones as the program has been improved. When comparing the effective doses calculated with the ODS-60 version based on the bone correction method described in this thesis, the differences between calculations and measurements are 10 %, 18 % and 2 % for chest posteroanterior (PA), abdomen anteroposterior (AP) and modified lumbar spine lateral (LAT) projections, respectively. Table I summarises the comparison of doses calculated with different ODS-60 versions to the measured doses.

The ability to use a patient specific dose calculation method provides the means to draw a correlation between patient doses and patient characteristics, i.e. size and sex. The benefit from using the patient specific doses can be seen from figure 2 in Publ. II, where the conversion from dose-area product, DAP, to $\mathcal{E}$ is presented as a function of patient sex and weight. The equations obtained for the conversion were

$$\mathcal{E}/DAP = 0.92\ e^{-0.0154\ weight} \tag{3a}$$

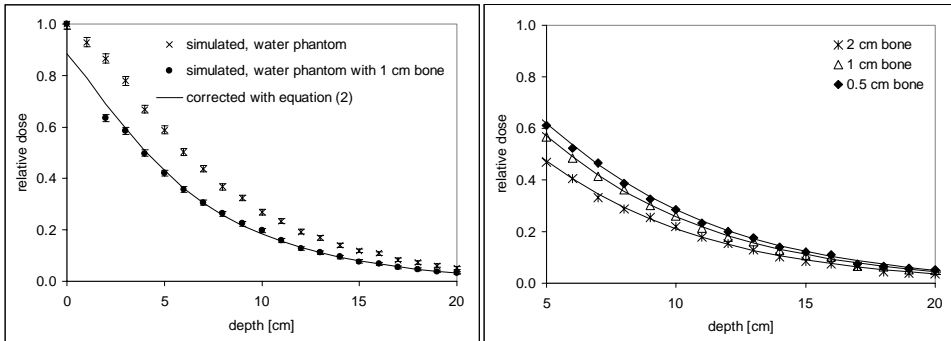$$\mathcal{E}/DAP = 0.56\ e^{-0.0154\ weight} \tag{3b}$$

Figure 2. The graph on the left shows the correction method applied to an X-ray spectrum (Birch et al. 1979) for 100 kV of tube voltage and 3 mm Al of filtration and a 10-mm thick bone layer. On the right, the correction method applied for different bone thickness is shown (50 keV monoenergetic beam). In both figures, the lines represent the depth dose curves derived using the correction method. Error bars in the left figure indicate the statistical error of the Monte Carlo simulation.

Table I. Comparison of effective doses calculated with different ODS-60 versions and measured in an Alderson-Rando phantom. Effective doses [mSv] and the relative difference of calculated and measured effective doses (in parentheses) are given. Entrance surface doses used in the comparison do not correspond to real examinations.

Method Reference	Measured Toivonen et al. (1996)	ODS-60 v1.0 Publ I	ODS-60 v2.0 Publ II	ODS-60 v2.1 this thesis
chest PA	21	25 (19 %)	23 (7 %)	19 (10 %)
abdomen AP	22	28 (27 %)	27 (23 %)	26 (18 %)
mod. lumbar spine LAT	10	11 (10 %)	10 (1 %)	9.8 (2 %)

where weight is given in kg, for females and males, respectively. The equations above are derived from doses calculated for 89 adult patients and therefore should not be used for paediatric patients. The phantom transformation (Servomaa et al. 1989) is valid from 40 to 110 kg and 140 to 200 cm sized patients.

In Table V of Publ. II, the $\mathcal{E}/DAP$ [mSv/Gy·cm^2] conversion was compared to a conversion coefficient derived using a MIRD phantom by Hart et al. (1994) and to sex specific conversion coefficients by Geleijns et al. (1997). The relative standard deviation (S.D.) of the difference between doses derived from coefficients and the actual doses was 39 % for 0.28 mSv/Gy·cm^2 from Hart et al. (1994). For Geleijns et al. (1997) S.D. was 27 % for females (0.33 mSv/Gy·cm^2) and 25 % for males (0.20 mSv/Gy·cm^2). The relative standard deviation of the conversion using equations 3a and 3b was 16 % for females (0.38 mSv/Gy·cm^2 for 58 kg) and 21 % (0.19 mSv/Gy·cm^2 for 70 kg) for males. In general, the mean and median of the differences between patient specific doses and those obtained with different conversion coefficients or functions are comparable with each other. This indicates that all calculation methods deliver similar doses for an average patient.

The factors behind the variation of the doses of the 89 barium enema patients were analysed in Publ. III. The median effective doses in the five hospitals were 4.4, 6.1, 7.1, 13 and 16 mSv. When compared with each other, the effective dose distributions in the hospitals were significantly different. Only the E in one hospital was not different from E in three others due to a wide distribution of E in that hospital. The correlation analysis showed that 40 % of the variation could be explained with radiologist controlled factors, i.e. screening time and number of exposures. Only 16 % of the variation was related to patient characteristics, i.e. patient weight and height, sex and age. The residual 44 % includes e.g. the equipment-related factors.

An interesting finding in the correlation analysis was that both patient's weight and height correlated negatively with effective dose. This phenomenon was studied in Publ. II where the functionalities of the exposure control equipment in the hospitals were analysed theoretically. Our findings were in agreement with an earlier result by Rowley et al. (1987) that the exposure control equipment is reaching the limits of its capability at

the extremes of patient weights. Even for an individual patient the exposure control may deliver exposures with hundred-fold differences.

The great variation of exposures indicates that exposure control equipment is not used optimally, i.e. either bone or contrast media (barium) is disturbing the measurement sensor of the exposure control. This should be avoided by using those measurement sensors that are not shadowed by bone or contrast media.

3 CALCULATING INTERNAL PATIENT RADIATION DOSE IN NUCLEAR MEDICINE

A computer program, later referred to as Intdose, was developed to calculate absorbed dose distribution in patient administered radiopharmaceuticals for diagnostic or therapeutic purposes. The calculation is based on a convolution process implemented with a Fast Fourier transformation (FFT) in 3 dimensions. The program code was written in standard C language and compiled with Gnu Project C Compiler (gcc).

Images from two distinct imaging modalities are needed in order to calculate absorbed dose distribution in the patient and to use the distribution to calculate the mean absorbed dose to an organ. In single photon emission computed tomography (SPECT) multiple acquisitions from the region of interest (ROI) are registered from different angles. These planar views are then used to construct a 3 dimensional count matrix relative to the activity distribution in that volume. The count matrix is then converted to an activity matrix by some quantification method. Magnetic resonance (MR) or computed tomography (CT) images of the patient are also needed, because SPECT images do not contain direct anatomical information. The SPECT and MR or CT images must be presented in the same co-ordinate system; i.e. the images must be registered.

3.1 Methods

The Intdose has two separate modules, the first calculating dose distribution in the co-ordinate system (matrix) of the images and the second calculating the mean absorbed dose in the voxels of each organ. The calculation of the dose distribution is based on convoluting the activity matrix with a point dose kernel matrix. The point dose kernel describes how radiation absorbs to a medium as a function of distance from a point source of certain isotope per one decay. Point dose kernels are produced with Monte Carlo simulations and have been published by e.g. Furhang et al. (1996b). The result of the convolution process is an activity distribution weighted sum of point dose kernels, i.e. the dose rate distribution. A straightforward convolution of two e.g. 128x128x128 (about $2 \cdot 10^6$ voxels) sized matrices would be an enormous task. A novel method to achieve the same result is to use Fast Fourier transform (FFT). The concept of the Fourier transform is that convolutions in one space correspond to multiplications in the reciprocal space (Webb 1988). Using FFT, the calculation of the dose date distribution $dD/dt(\boldsymbol{r})$ may be formulated as

$$dD/dt(\boldsymbol{r})=FFT^{-1}[FFT\{A(\boldsymbol{r})\}\cdot FFT\{K(\boldsymbol{r})\}] \tag{4}$$

where $A(r)$ is the activity distribution, $K(r)$ is the point dose kernel and the notation FFT^{-1} means the inverse of Fast Fourier transform. The dose rate distribution may subsequently be converted in to a dose distribution, $D(r)$, by using the physical half-life of

the nuclide in question. The dose contribution from β-decays (Browne et al. 1986) was assumed to be local within the source voxels.

A phantom study was carried out to compare the absorbed doses measured with thermoluminescent (TL) detectors and those calculated with Intdose (Publ. V). The phantom was an elliptical water phantom[5] with a cylindrical ^{131}I source. The activity distribution was generated by hand to correspond to the known location (focal point or centre of the phantom), dimensions (diameter 5.3 cm and height 8 cm) and activity (3000 MBq) of the source.

The clinical applicability of Intdose was demonstrated in Publ. IV by calculating absorbed doses to liver and spleen for three healthy volunteers administered two common radiopharmaceuticals used in diagnostics. The volunteers were first administered ^{111}In-oxine-labeled thrombocytes and two days later ^{99m}Tc-labeled tin colloids (Pohjonen et al. 1996). The MR images of the volunteers were registered with SPECT images describing the count distribution after the administration of each radiopharmaceutical. The MR images were segmented to identify the spleen and liver. The imaging and registration protocols are described in detail by Pohjonen et al. (1996). The errors associated with the registration procedure used in Publ. IV are discussed by Sipilä et al. (1997). The local ethical committee approved the study and informed consent was obtained from all volunteers. The activity distribution was calculated from the count matrix by assuming that all activity was present in the imaged volume and that the activity in each voxel was linearly dependent on the number of counts.

As part of a study describing a method for determining absorbed doses to organs in systemic radiation therapy (SRT), doses to patients' kidneys were calculated using the Intdose program (Publ. V). The method described was based on thermoluminescent (TL) detectors placed on the patient's skin. Doses to the kidneys of six patients treated with SRT were determined with the TL method, Intdose and MIRD formalism (MIRDOSE3 program).

The SRT patients had large intraperitoneal disease (pseudomyxoma) with no exact tumour volume. The patients were administered ^{131}I-ladeled monoclonal antibody (MoAb) intraperitoneally. CT and SPECT images were taken from the abdominal area of the patients. SPECT imaging was performed at 3, 10 and 24 days after injection.

The count matrix used in the dose distribution calculation by Intdose was taken from the third-day SPECT images. All the activity administered was assumed to be located in the volume covered by the SPECT images. The CT and SPECT images were not registered and external markers to enable this were not used. The images were transformed to the same co-ordinate system by hand using i.e. scout images. Also, the original CT images, which consisted of 1 cm thick 256x256 slices (pixel size 2.0x2.0 mm), were transformed to equal the format of the SPECT data (9.34 mm thick 64x64 slices with pixel size of 5.76x5.76 mm). The point dose kernel for ^{131}I was taken from Furhang et al. (1996b). Although the CT and SPECT images were presented in a 64x64x64-sized

---

[5] Data Spectrum Corporation, Hillsborough, North Carolina, USA

matrix, they were embedded in 128x128x128-sized zero matrixes in order to prevent the folding of the Fourier transform (Press et al. 1992).

3.2 Results and findings

According to the phantom study in Publ. V, Intdose agreed within 3 % with the measurements inside the water phantom. The phantom calculation used ideal and known activity distribution and therefore did not have the uncertainties of the SPECT activity quantitation present. The resulting 3 % difference between the measurements and calculations may be regarded as proof of applicability of the convolution method.

In Publ. IV the mean absorbed doses to livers and spleens of the volunteers calculated with Intdose were compared to those given in ICRP Publication 53 (ICRP 1987). On average, the results were in good agreement, as can be seen from table 1 in Publ. IV. In case of ^{99m}Tc, the difference of the mean absorbed dose to liver per activity administered, calculated by Intdose and given by ICRP (1987) is 8 %. In case of ^{111}In and spleen, the difference is 20 %. Variation in the patient specific doses to the organs of the volunteers is explained with variable organ sizes.

In addition to organ doses, the S-values $S(_{liver-spleen})$, $S(_{liver-liver})$, $S(_{spleen-liver})$ and $S(_{spleen-spleen})$ were also calculated and compared to those given by MIRDOSE3 (Stabin 1996). In general, the S-values agree well in cases where the target organ is also the source, i.e. $S(_{liver-liver})$ and $S(_{spleen-spleen})$. For ^{99m}Tc, the average $S(_{liver-liver})$ and $S(_{spleen-spleen})$ calculated by Intdose differ by 7 % and 3 %, respectively, from those given by MIRDOSE3. For ^{111}In, the corresponding differences are 3 % and 25 %. In other cases the agreement is within the order of magnitude. The differences in S-values are also mainly due to different organ sizes. For example, the ratio of the spleen sizes of volunteers 2 and 3 is 2.8 (Pohjonen et al. 1996).

For kidney doses of eight SRT patients, a general trend between the doses determined with the TL method and those calculated with either Intdose or MIRDOSE3 was that the calculated doses were higher. Calculated (Intdose) absorbed doses to the right kidney varied from 89 to 235 µGy/MBq (mean 158 µGy/MBq) and correspondingly from 89 to 216 µGy/MBq (mean 157 µGy/MBq) to the left kidney. The doses were, on average, 93 % and 100 % higher than those derived with the TL method. The residence times used in the calculations were taken from daily gamma images. According to gamma images, the average effective half-live of the radiopharmaceuticals in the peritoneal cavities of the patients was 27 hours (physical half-life of ^{131}I is 8.04 days). The calculations were done on the basis of the activity (count) distribution on the third day. Even though the patient specific effective half-lives were used, the assumption of a constant activity distribution was not adequate. A better result would require using more than one set of SPECT images in the calculations. On the other hand, the overall uncertainty of the TL method was 46 % (1 standard deviation). As concluded in Publ. V, in terms of dose calculations, ^{131}I is a sub-optimal choice for systemic radiation therapy.

4   DISCUSSION

Two computer programs aimed for patient dosimetry purposes and their applicability in clinical examinations were presented in this thesis. Both programs calculate organ doses for individual patients using patient specific calculation phantoms.

Awareness of the risks associated with ionising radiation has lead to a need to estimate these risks at the level of an individual patient. It is remarkable that there is no such quantity defined, which could be used to characterise radiation detriment for an individual patient. The effective dose, E, is intended for radiation protection purposes only and should not be used for individual patients. The weighting factors are statistically derived from a large population. The properties of individual patient's organs and tissues may differ from those of a large population. It is impossible to determine individual weighting factors, i.e. quantities related to individual probabilities for radiation-induced cancer or genetic alteration. It is, however, possible to derive weighting factors for smaller sub-groups, for example for females and males separately as well as for children and adolescents (Almén et Mattsson 1996). These dependencies have also been considered in the BEIR V report (BEIR 1990).

The effective individual dose $\mathcal{E}$ introduced in Publ. II uses the same values for weighting factors as the effective dose E does. The only difference between these two quantities is that the contribution of those organs not present in the sex-specific phantom is not accounted for. Therefore, $\mathcal{E}$ does not include any additional patient specific factors but sex. In order to include the effect of e.g. patient's age into $\mathcal{E}$, new weighting factors including these dependencies are needed. However, a simple modification to the values of the present weighting factors may be used to estimate the radiation-related risk to the non-fertile patients. For this group, only somatic risk is relevant, i.e. genetic risk may be neglected. An example of this is given in Publ. II, where sex specific risk estimates, assuming that the patients are not fertile, are also given for barium enema examination patients.

Conversion coefficients are useful tools for making estimations about the organ and effective doses from an exposure. Since the effective dose is a quantity to be used in population risk assessments, the input parameters used in conversion should also be averages from a large number of examinations, i.e. corresponding to an average examination procedure. One application of these whole population averaged effective doses is the determination of collective doses. The effective doses resulting from the conversion are valid for the phantom for which the conversion coefficient has been derived. In case of the MIRD phantom, its properties are considered to correspond to those of an average human. Since the MIRD phantom was originally designed for dosimetry of internal sources, its development has focused on correct centre-of-mass distances of different organs instead of correct anatomical shapes or positions. When applied to dosimetry of internal sources, the MIRD phantom is realistic. However, when applied to dosimetry of external radiation with limited field sizes, the locations and shapes of the organs in relation to the radiation field are of importance.

The concept of converting an easily measurable quantity to another quantity relating to radiation induced risk, is elegant. To improve the accuracy of the presently used MIRD phantom based conversion coefficients (e.g. Hart et al. 1994), the conversions for simple X-ray examinations should be re-determined from limited patient samples using a patient specific calculation method, e.g. ODS-60 program presented in this thesis. As an example, conversion equations derived for barium enema examinations using ODS-60 (equations 3a and b), give about a 50 % smaller standard deviation for the ratio of the actual and converted effective doses than the method using Monte Carlo simulation and the MIRD phantom (Hart et al. 1994). For those examinations and procedures not favouring the use of simple conversion, because of highly individual exposures, one should use the patient specific calculation application itself. Whether ODS-60, or any other patient specific dose calculation method, is used for re-producing conversion functions or for truly individual patient specific dose determination, the effective dose should be redefined to allow the calculation of individual risk related quantity.

The main concern in radiation protection proclamation by ICRP has been focused on the societal criteria, i.e. collective doses have been used to determine the optimum spend on the control of a source (Clarke 1998). The discussion aimed to change this approach to a more individual-based philosophy has been opened by R. Clarke (1998), chairman of ICRP. The proposed schema includes a concept of a *controllable dose*, which could be derived for individuals. The specific methods for determining, i.e. measuring or calculating, these *controllable doses* are still unknown. Whatever the means of determination are, the equation must include individual organ doses, if truly individual radiation detriment related quantities are desired.

Organ doses are measurable quantities, at least indirectly, and may be determined for individual patients. In practise, the measurement method must be based on recording of the parameters of the exposure and some calculation algorithm to assess the organ doses. The desired accuracy of the organ doses determines what requirements the details of the recorded exposure parameters and patient characteristics must meet. For simple examinations with small effective (individual) dose, i.e. a thorax posteroanterior (PA) X-ray examination, it is adequate to estimate the dose with, for example, a *DAP* measurement and a conversion coefficient or function. The main interest areas for accurate dose determinations are the examinations and procedures with high doses, i.e. examinations and operations using fluoroscopy screening, especially interventional radiology.

The manual recording of the exposure parameters needed for accurate organ dose calculations of barium enema examinations required two dedicated people. Although possible in scientific studies, it is naturally out of the question in clinical routine. Therefore, as much of the recording should be automated as possible. A device measuring air kerma, dimensions of the X-ray field and focus-skin distance, e.g. one proposed by Rannikko et Helenius (1998), in addition to field location and projection sensing equipment would be needed. The latter should be built internally to the X-ray equipment as well as the sensors for X-ray beam quality.

The problems in the dosimetry of radiopharmaceuticals are different from those of external radiation. Once the radiopharmaceutical has been administered, it distributes in the blood, tissues and organs of the patient. This biodistribution is highly patient specific. In fact, the diagnostic use of a radiopharmaceutical is based on observing the patient specific biodistribution and with knowledge of normal distribution, the physician is able to assess the internal condition of the patient. In therapy applications the requirements for accurate dosimetry are emphasised, since the absorbed dose in the dose limiting healthy organs must be kept below dose limits. In therapy, the biodistribution is even more difficult to predict than in diagnostics, since the radiopharmaceutical is usually labelled with a tumour specific antibody. Most of the radiopharmaceutical particles are likely to attach to the tumour cells, but the behaviour of the remaining part is unknown, it may, for example, circulate in the blood, concentrate to the thyroid or exit the system through the urinary system.

Single photon emission computed tomography (SPECT) imaging provides a 3-dimensional distribution of the measured counts. If this count distribution is to be used in the calculation of the dose distribution in a patient, two requirements may be set to the imaging protocol. First, the SPECT images should be registered with anatomical magnetic resonance (MR) or computed tomography (CT) images. Second, the count distribution should be quantified in terms of absolute activity. The methods for image registration are already available for clinical use (e.g. Pohjonen et al. 1996). The methods for absolute quantitation of SPECT images are available through attenuation and scatter corrections (Ljungberg 1990), which could be practically implemented using e.g. transmission imaging. In transmission imaging a multihead SPECT camera and a line source are used to acquire a crude transmission tomograph image of the patient. The tomograph is then used in the attenuation and scatter corrections. Kauppinen (1999) has presented an up-todate discussion about the scatter and attenuation corrections and SPECT image reconstruction.

Calculation applications for dosimetry of radiopharmaceuticals, as Intdose presented in this thesis, rely on accurate activity quantitation and image registration methods. The activity quantitation is the Achilles heel of all dose calculation methods using SPECT data to determine the activity distribution. In this respect Intdose does not bring new aspects to previous methods like MIRDOSE3 and S-values in general. The accuracy of the dose distribution calculated with Intdose is in principle only limited by the accuracy of the activity distribution. As seen from the phantom measurement in Publ. V, in calculations based on known activity distribution, the results agree with those from measurements within 3 %. The benefit of using Intdose instead of pre-calculated organ level S-values (e.g. ICRP 1987) is independence over pre-defined organs as sources and targets. Also, organ level S-values assume homogeneous activity distribution in a source organ and also the results are given as average absorbed doses in each organ.

In diagnostic imaging using radiopharmaceuticals it is not practical to obtain the anatomical information of the patient from MR or CT images. Therefore, a simplified version of the Intdose, calculating only dose distribution without corresponding ana-

tomical information, could be used in diagnostic applications if some estimate about the dose is needed. On the other hand, organ level S-values give in most cases adequate dose estimations for diagnostic patients. The main future use for full monty Intdose using also anatomical data is, without a doubt, in therapy applications where knowledge of the dose distribution is essential.

Although the effective dose is a weighted sum of the organ doses, the concept of mean absorbed dose in an organ may not be relevant in all occasions. A hot spot, i.e. a high local absorbed dose deposition, in an organ may, even though the average organ dose is low, cause necrosis in the organ. Examples of this are the acute radiation injuries experienced from locally high skin doses in interventional X-ray procedures (see e.g. Huda et Peters (1994), Vañó et al. (1998)). Because of the possibility for acute radiation symptoms for skin, the conversion coefficient method of measuring the pure total *DAP* value, without any information about field location, of an interventional procedure, is of little value. Instead of the average organ doses, a peak absorbed dose value on patient's skin should be known. The ODS-60 program presented in this thesis is an example of the software part of a method able to assess absorbed dose distribution on patient's skin as a side product of organ doses. Analogously, in dosimetry of radiopharmaceuticals, Intdose may be used to examine the dose distribution in an organ to discover the hot and cold spots.

The computer applications presented in this thesis, ODS-60 for dosimetry of X-ray examinations and Intdose for dosimetry of radiopharmaceuticals, are practical solutions to fulfil the growing demands for patient specific dosimetry. In practice, ODS-60 can be used in two ways. First, to produce more realistic conversion equations for simple X-ray examinations than the presently used conversion coefficients from Monte Carlo simulations using a MIRD phantom. Second, to calculate individual patient specific organ and effective doses in those X-ray examinations and procedures which involve non-standard exposures making the use of conversion equations impracticable. As for Intdose, its use is most advantageous in therapy applications. In radiopharmaceutical diagnostics the use of the established organ level S-values is the practical solution to dose assessments. In therapy, however, Intdose's ability to use patient specific activity distribution and anatomical data in addition to the ability to examine the resulting dose distribution makes it superior to pre-calculated S-values.

ACKNOWLEDGEMENTS

Järvenpää, February 2000   Juha Lampinen

REFERENCES

Andreo P. Monte Carlo techniques in medical radiation physics. Phys Med Biol 1991; 36: 861-920.

Almén A, Mattsson S. On the calculation of effective dose to children and adolescents. J Radiol Prot 1996; 16: 81-89.

Attix FH. Introduction to radiological physics and radiation dosimetry. New York: John Wiley & Sons, 1986.

Briesmeister JF (ed.). MCNP - A General Monte Carlo N-Particle Transport Code. Los Alamos National Laboratory Report LA-12625-M, 1997.

Bolch WE, Bouchet LG, Robertson JS, Wessels BW, Siegel JA, Howell RW, Erdi AK, Aydogan B, Costes S, Watson EE, Brill AB, Charkes ND, Fisher DR, Hays MT, Thomas SR. The dosimetry of nonuniform activity distributions-radionuclide S values at the voxel level. Medical Internal Radiation Dose Committee (MIRD) Pamphlet No. 17. J Nucl Med 1999; 40(1): 11S-36S.

Birch R, Marshall M, Ardran GM. Catalogue of spectral data for diagnostic X-rays. London: Hospital Physicist's Association, 1979.

Boone JM, Seibert JA. An accurate method for computer-generating tungsten anode x-ray spectra from 30 to 140 kV. Med Phys 1997; 24(11):1661-70.

Browne E, Firestone RB, Shirley VS. Table of radioactive isotopes. New York, John Wiley & Sons, 1986.

Clarke R. Control of low-level radiation exposure: time for a change? J Radiol Prot 1998; 19: 107-115.

Committee on the Biological Effects of Ioninizing Radiation. Health effects of exposure to low levels of ionizing radiation. BEIR V. Washington: National Academy Press, 1990.

Cristy M. Mathematical phantoms representing children of various ages for use in estimates of internal dose. NUREG/CR-1159. Tennessee: ORNL, 1980.

Drexler G, Panzer W, Widenmann L, Williams G, Zankl M. The calculation of dose from external photon exposures using human phantoms and Monte Carlo methods. Part III: Organ doses in X-ray diagnostics. GSF-Report S-1026. München: Gesellschaft für Strahlen und Umweltforschung mbH, 1984.

European Commission (EC). Council Directive 97/43/Euratom of 30 June 1997 on health protection of individuals against the dangers of ionising radiation in relation to medical exposures, and repealing Directive 84/466/Euratom. Official Journal of the European Communities 1997; 9.7.97 No L180: 22–27.

Furhang EE, Chui CS, Sgouros G. A Monte Carlo approach to patient-specific dosimetry. Med Phys 1996a; 23: 1523-1529.

Furhang EE, Sgouros G, Chui C-S. Radionuclide photon dose kernels for internal dosimetry. Med Phys 1996b; 23: 759-764.

Furhang EE, Chui CS, Kolbert KS, Larson SM, Sgouros G. Implementation of a Monte Carlo dosimetry method for patient-specific internal emitter therapy. Med Phys 1997; 24: 1163-1172.

Geleijns J, Broerse JJ, Shaw MP, Schultz FW, Teeuwisse W, van Unnik JG, Zoetelief J. Patient dose due to colon examination: dose assessment and results from a survey in The Netherlands. Radiology 1997; 204(2): 553-559.

Grosswendt B. Dependence of the photon back-scatter factor for water on source-to-phantom distance and irradiation field size. Phys Med Biol 1990; 35: 1233-1245.

Hart D, Jones DG, Wall BF. Estimation of effective dose in diagnostic radiology from entrance surface dose and dose-area product measurements. National Radiological Protection Board, NRPB-R262. London: HMSO, 1994.

Hart D, Jones DG, Wall BF. Coefficients for estimating effective doses from paediatric X-ray examinations. National Radiological Protection Board, NRPB-R279. London: HMSO, 1996.

Howell RW, Wessels BW, Loevinger R, Watson EE, Bolch WE, Brill AB, Charkes ND, Fisher DR, Hays MT, Robertson JS, Siegel JA, Thomas SR. The MIRD perspective 1999. Medical Internal Radiation Dose Committee. J Nucl Med 1999; 40(1): 3S-10S.

Hubbell JH, Seltzer SM. Tables of X-ray mass attenuation coefficients and mass energy-absorption coefficients from 1 keV to 20 MeV for elements Z = 1 to 92 and 48 additional substances of dosimetric interest. http://physics.nist.gov/PhysRefData/XrayMassCoef, 1997.

Huda W, Peters KR. Radiation-induced temporary epilation after a neuroradiologically guided embolization procedure. Radiology 1994; 193: 642-644.

International Commission on Radiological Protection (ICRP). Radiation dose to patients from radiopharmaceuticals. ICRP Publication 53. Oxford: Pergamon Press, 1987.

International Commission on Radiological Protection (ICRP). 1990 Recommendations of the International Commission on Radiological Protection. ICRP Publication 60. Oxford: Pergamon Press, 1991.

International Commission on Radiological Protection (ICRP). Age-dependent doses to members of the public from intake of radionuclides: Part 4, Inhalation dose coefficients. ICRP Publication 71. Oxford: Pergamon Press, 1995.

Johnson TK. MABDOS: A generalized program for internal radionuclide dosimetry. Comput Methods Programs Biomed 1988; 27: 159-167.

Jones DG, Wall BF. Organ doses from medical X-ray examinations calculated using Monte Carlo techniques. National Radiological Protection Board, NRPB-R186. London: HMSO, 1985.

Kauppinen T. Improvement of SPET imaging using iterative reconstruction (dissertation). Kuopio University Publications C. Natural and Environmental Sciences 101. Kuopio: Kuopio University, 1999.

Kawrakow I, Fippel M, Friedrich K. 3D electron dose calculation using a Voxel based Monte Carlo algorithm (VMC). Med Phys 1996; 23(4): 445-457.

Kramer R, Zankl M, Williams G, Drexler G. The calculation of dose from external photon exposures using reference human phantoms and Monte Carlo methods. Part I: The male (ADAM) and female (EVA) adult mathematical phantoms. GSF-Report S-885. München: Gesellschaft für Strahlen und Umweltforschung mbH, 1982.

Lampinen J, Rannikko S, Savolainen S. A computer program for the on line registration of the exposure data of x-ray examinations. Med & Biol Eng & Comput 1996; 34, suppl 1, part 1: 213-214.

Ljungberg M. Development and evaluation of attenuation and scatter correction techniques for SPECT using the Monte Carlo method (dissertation). Lund: University of Lund, 1990.

Loevinger R, Berman M. A schema for absorbed-dose dose calculation for biologically distributed radionuclides. Medical Internal Radiation Dose Committee (MIRD) Pamphlet No. 1. J Nucl Med 1968; 9, suppl 1: 7-14.

Nelson WR, Hirayama H, Rogers DWO. The EGS4 code system. Stanford Linear Accelerator Center Report SLAC-265, 1985.

du Plessis FC, Willemse CA, Lotter MG, Goedhals L. The indirect use of CT numbers to establish material properties needed for Monte Carlo calculation of dose distributions in patients. Med Phys 1998; 25(7 pt 1); 1195-1201.

Pohjonen HK, Savolainen SE, Nikkinen PH, Poutanen V-PO, Korppi-Tommola ET, Liewendahl BK. Abdominal SPECT/MRI fusion applied to the study of splenic and hepatic uptake of radiolabeled thrombocytes and colloids. Ann Nucl Med 1996; 10: 409-417.

Press WH, Teukolsky SA, Vetterling WT, Flannery BP. Numerical recipes in C: The art of scientific computing, 2nd ed. Cambridge: Cambridge Press, 1992.

Rannikko S, Karila KTK, Toivonen M. Patient and population doses of X-ray diagnostics in Finland. STUK-A144. Helsinki: Oy Edita Ab, 1997.

Rannikko S, Helenius K. Method and apparatus for determining the field size and the field form of the radiation cone of ionizing radiation source. United States Patent, no:5, 760, 404, 1998.

Rosenstein M. Handbook of selected organ doses for projections in diagnostic radiology. Food and Drug Administration, FDA. HEW Publication 76-8031. Rockville, MD: HEW, 1976.

Rosenstein M, Beck T, Warner GG. Handbook of selected organ doses for projections common in paediatric radiology. Food and Drug Administration, FDA. HEW Publication 79-8079. Rockville, MD: HEW, 1979.

Rowley KA, Hill SJ, Watkins RA, Moores BM. An investigation into the levels of radiation exposure in diagnostic examinations involving fluoroscopy. Br J Radiol 1987; 60: 167-173.

Schroeder L. Buffon's needle problem: An exciting application of many mathematical concepts. Mathematics Teacher 1974; 67: 183-186.

Servomaa A, Rannikko S, Nikitin V, Golikov V, Ermakov I, Masarskyi L, Saltukova L. A topographically and anatomically unified phantom model for organ dose determination in radiation hygiene. STUK-A87. Helsinki: Painatuskeskus Oy, 1989.

Sipilä O, Nikkinen P, Pohjonen H, Poutanen V-P, Visa A, Savolainen S, Katila T, Liewendahl K. Accuracy of a registration procedure for brain SPECT and MRI: Phantom and simulation studies. Nucl Med Commun 1997; 18: 517-526.

Snyder WS, Ford MR, Warner GG, Fisher HL. Estimates of absorbed fractions for monoenergetic photon sources uniformly distributed in various organs of a heterogeneous phantom. Medical Internal Radiation Dose Committee (MIRD) Pamphlet No. 5. J Nucl Med 1969; 10, suppl. 3: 7-14.

Snyder WS, Ford MR, Warner GG, Watson SB. "S": absorbed dose per unit cumulated activity for selected radionuclides and organs. Medical Internal Radiation Dose Committee (MIRD) Pamphlet No. 11. New York: The Society of Nuclear Medicine, 1975.

Stabin MG. MIRDOSE: Personal computer software for internal dose assessment in nuclear medicine. J Nucl Med 1996; 37: 538-546.

Symington J. An atlas illustrating the topographical anatomy of the head, neck and trunk. Edinburgh: Olivar and Boyd, 1956.

Tagesson M, Ljungberg M, Strand SE. A Monte-Carlo program converting activity distributions to absorbed dose distributions in radionuclide treatment planning system. Acta Oncol 1996; 35(3): 367-372.

Tapiovaara M. Handbook of physics in X-ray diagnostics, part II: Patient doses. STL-B54 (in Finnish). Helsinki: Institute of Radiation Protection, 1983.

Tapiovaara M, Lakkisto M, Servomaa A. PCXMC - A PC-based Monte Carlo program for calculating patient doses in medical x-ray examinations. STUK-A139. Helsinki: Oy Edita Ab, 1997.

Toivonen M, Aschan C, Rannikko S, Karila K, Savolainen S. Organ dose determinations of X-ray examinations using TL detectors for verification of computed doses. Rad Prot Dosim 1996; 66: 289-294.

Vañó E, Arranz L, Sastre JM, Moro C, Ledo A, Gárate MT, Minguez I. Dosimetric and radiation protection considerations based on some cases of patient skin injuries in interventional cardiology. Br J Radiol 1998; 71: 510-516.

Webb S (ed.). The physics of medical imaging. Bristol: Institute of Physics Publishing, 1988.